

Cosmological evolution of a Peccei-Quinn field with small self-coupling and implications for Axion Dark Matter

Paweł Kozów

University of Warsaw

*Theory and Experiment in High Energy Physics
Czech Technical University in Prague, 3 October 2024*

based on PK, M. Olechowski, JCAP 06 (2023) 043

- 1 **Introduction**
- 2 Radiative corrections
- 3 ϕ evolution during inflation – geometric corrections
- 4 ϕ evolution after inflation – thermal corrections
- 5 Numerical Results: influence of each correction on axion relics
- 6 Summary and Conclusions

- **Axions (QCD axions and ALPs)**

- pseudo Goldstone bosons of spontaneously broken Peccei-Quinn global $U(1)_{PQ}$ symmetry
- phase component of complex PQ scalar

$$\Phi = \frac{1}{\sqrt{2}} S e^{ia/f_a} = \frac{1}{\sqrt{2}} S e^{i\theta}$$

- $U(1)_{PQ}$ is anomalous and axion potential is developed (non-perturbatively) long after inflation

$$V_a \sim m_a^2 f_a^2 \left(1 - \cos \frac{a}{f_a} \right) = m_a^2 f_a^2 (1 - \cos \theta)$$

Axions are interesting candidates for Dark Matter

$$V(\Phi) = \lambda_\Phi \left(|\Phi|^2 - \frac{f_a^2}{2} \right)^2 = \frac{\lambda_\Phi}{4} (S^2 - f_a^2)^2, \quad m_S^2 = 2\lambda_\Phi f_a^2$$

Two basic scenarios:

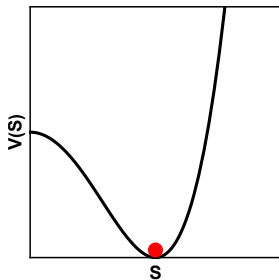
Axions are interesting candidates for Dark Matter

$$V(\Phi) = \lambda_\Phi \left(|\Phi|^2 - \frac{f_a^2}{2} \right)^2 = \frac{\lambda_\Phi}{4} (S^2 - f_a^2)^2, \quad m_S^2 = 2\lambda_\Phi f_a^2$$

Two basic scenarios:

(i) $m_S \gg H_I$ (' $U(1)_{PQ}$ broken')

- $S = f_a$ during and after inflation
- θ_i determined by some stochastic process
(the phase transition from unbroken to broken $U(1)_{PQ}$)
- \Rightarrow If θ_i not aligned with the minimum of V_a
Axion starts oscillating when $H \lesssim \frac{1}{3}m_a$
 \rightarrow cold dark matter (CDM)



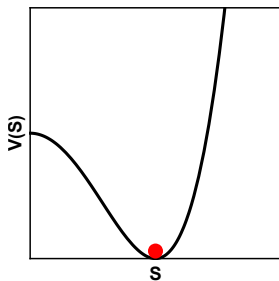
Axions are interesting candidates for Dark Matter

$$V(\Phi) = \lambda_\Phi \left(|\Phi|^2 - \frac{f_a^2}{2} \right)^2 = \frac{\lambda_\Phi}{4} (S^2 - f_a^2)^2, \quad m_S^2 = 2\lambda_\Phi f_a^2$$

Two basic scenarios:

(i) $m_S \gg H_I$ (' $U(1)_{PQ}$ broken')

- $S = f_a$ during and after inflation
- θ_i determined by some stochastic process
(the phase transition from unbroken to broken $U(1)_{PQ}$)
- \Rightarrow If θ_i not aligned with the minimum of V_a
Axion starts oscillating when $H \lesssim \frac{1}{3}m_a$
 \rightarrow cold dark matter (CDM)



Axion field a is massless during inflation \Rightarrow it has stochastic quantum fluctuations: a changes on average by $H_I/2\pi$ during each Hubble time, in each Hubble volume

- θ has dispersion $\langle \delta\theta_i^2 \rangle$, generated by quantum fluctuations during inflation
 \Rightarrow Isocurvature perturbations of axion CDM $\langle \delta\theta_i^2 \rangle \propto (H_I/f_a)^2 \ll 1$

(ii) $m_S \ll H_I$

If saxion field S is light enough it also fluctuates during inflation

During inflation stochastic fluctuations of a light field "compete" with classical evolution caused by its potential

→ After long enough time the system approaches the Fokker-Planck probability distribution: $P_{\text{eq}}(\Phi) \propto \exp\left(-\frac{8\pi^2}{3} \frac{V(\Phi)}{H_I^4}\right)$ [Starobinsky, Yokoyama '94]

(ii) $m_S \ll H_I$

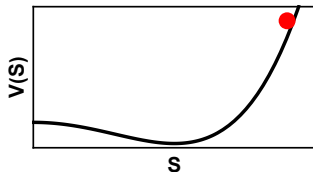
If saxion field S is light enough it also fluctuates during inflation

During inflation stochastic fluctuations of a light field "compete" with classical evolution caused by its potential

→ After long enough time the system approaches the Fokker-Planck probability distribution: $P_{\text{eq}}(\Phi) \propto \exp\left(-\frac{8\pi^2}{3} \frac{V(\Phi)}{H_I^4}\right)$ [Starobinsky, Yokoyama '94]

After (long enough) inflation:

- initial value of saxion field S_i (and θ_i) is determined by stochastic quantum fluctuations (ambiguity of S_i)
- the fields have dispersions, $\langle \delta S_i^2 \rangle$ and $\langle \delta \theta_i^2 \rangle$, generated by the stochastic quantum fluctuations during the last ~ 50 e-folds of inflation



(ii) $m_S \ll H_I$

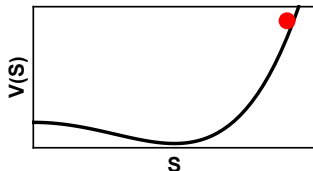
If saxion field S is light enough it also fluctuates during inflation

During inflation stochastic fluctuations of a light field "compete" with classical evolution caused by its potential

→ After long enough time the system approaches the Fokker-Planck probability distribution: $P_{\text{eq}}(\Phi) \propto \exp\left(-\frac{8\pi^2}{3} \frac{V(\Phi)}{H_I^4}\right)$ [Starobinsky, Yokoyama '94]

After (long enough) inflation:

- initial value of saxion field S_i (and θ_i) is determined by stochastic quantum fluctuations (ambiguity of S_i)
- the fields have dispersions, $\langle \delta S_i^2 \rangle$ and $\langle \delta \theta_i^2 \rangle$, generated by the stochastic quantum fluctuations during the last ~ 50 e-folds of inflation



This non-trivial dynamics after inflation may lead to production of a as

- cold dark matter, e.g. kinetic misalignment mechanism e.g. [Co, Harigaya, 19']
- warm dark matter (WDM), e.g. parametric resonance production e.g. [Harigaya et al 15']
 - Bounds on isocurvature perturbations lead to very strong upper bounds on the self-coupling, $\lambda_\phi \lesssim 10^{-20} \lll 1$ (flat potentials motivated by SUSY)

If $\lambda_\phi \lll 1$ one should consider corrections

- I. radiative
- II. geometric (curvature of space-time)
- III. thermal

In this talk I will concentrate on (ii) $m_S \ll H_I$, i.e. models in which PQ field has nontrivial dynamics during and after inflation

The goal is to check influence of I, II, III on axion contribution to CDM and WDM

- 1 Introduction
- 2 Radiative corrections**
- 3 ϕ evolution during inflation – geometric corrections
- 4 ϕ evolution after inflation – thermal corrections
- 5 Numerical Results: influence of each correction on axion relics
- 6 Summary and Conclusions

I. Radiative corrections (Coleman-Weinberg (CW) potential):

We adopt Gildener-Weinberg approach

- μ – scale at which running PQ self-coupling vanishes: $\lambda_\phi(\mu) = 0$

I. Radiative corrections (Coleman-Weinberg (CW) potential):

We adopt Gildener-Weinberg approach

- μ – scale at which running PQ self-coupling vanishes: $\lambda_\Phi(\mu) = 0$
- The PQ scalar Φ couples to some scalars ϕ_i and some fermions ψ_j

$$\mathcal{L} \supset - \sum_i \left(\frac{1}{2} m_i^2 \phi_i^2 + \frac{1}{2} \lambda_i |\Phi|^2 \phi_i^2 \right) - \sum_j y_j \Phi \bar{\psi}_j \psi_j$$

$$\rightarrow V_{CW}(\Phi) = \frac{1}{64\pi^2} \sum_{\text{scalars}} M_{\phi_i}^4 \left[\ln \left(\frac{M_{\phi_i}^2}{\mu^2} \right) - \frac{3}{2} \right] - \frac{4}{64\pi^2} \sum_{\text{fermions}} M_{\psi_j}^4 \left[\ln \left(\frac{M_{\psi_j}^2}{\mu^2} \right) - \frac{3}{2} \right]$$

$$M_{\phi_i}^2 = m_i^2 + \lambda_i |\Phi|^2, \quad M_{\psi_j}^2 = y_j^2 |\Phi|^2$$

I. Radiative corrections (Coleman-Weinberg (CW) potential):

We adopt Gildener-Weinberg approach

- μ – scale at which running PQ self-coupling vanishes: $\lambda_\Phi(\mu) = 0$
- The PQ scalar Φ couples to some scalars ϕ_i and some fermions ψ_j

$$\mathcal{L} \supset - \sum_i \left(\frac{1}{2} m_i^2 \phi_i^2 + \frac{1}{2} \lambda_i |\Phi|^2 \phi_i^2 \right) - \sum_j y_j \Phi \bar{\psi}_j \psi_j$$

$$\rightarrow V_{CW}(\Phi) = \frac{1}{64\pi^2} \sum_{\text{scalars}} M_{\phi_i}^4 \left[\ln \left(\frac{M_{\phi_i}^2}{\mu^2} \right) - \frac{3}{2} \right] - \frac{4}{64\pi^2} \sum_{\text{fermions}} M_{\psi_j}^4 \left[\ln \left(\frac{M_{\psi_j}^2}{\mu^2} \right) - \frac{3}{2} \right]$$

$$M_{\phi_i}^2 = m_i^2 + \lambda_i |\Phi|^2, \quad M_{\psi_j}^2 = y_j^2 |\Phi|^2$$

Simple model:

$$y_j = y, \quad \lambda_i = \lambda, \quad m_i^2 = m^2, \quad N_{\text{scalars}} = 4N_{\text{fermions}}$$

Bosonic contribution must dominate for large values of S

$$y^2 = (1 - \delta)\lambda, \quad 0 \leq \delta \leq 1$$

- **quasi-SUSY** when $\delta \ll 1$
- **SUSY limit:** $m \rightarrow 0$ and $\delta \rightarrow 0 \Rightarrow V_{CW} \rightarrow 0$

- 1 Introduction
- 2 Radiative corrections
- 3 Φ evolution during inflation – geometric corrections**
- 4 Φ evolution after inflation – thermal corrections
- 5 Numerical Results: influence of each correction on axion relics
- 6 Summary and Conclusions

II. Geometric corrections:

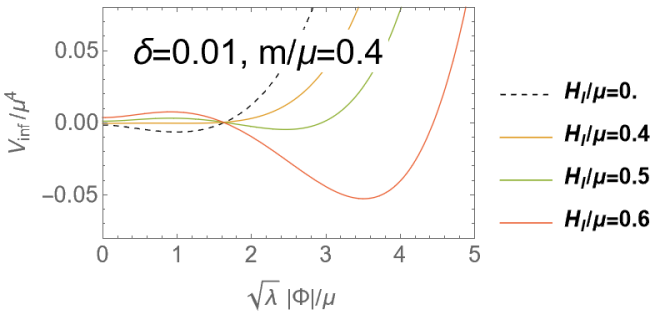
CW potential in curved space-time

[Markkanen, Nurmi, Rajantie, Stopyra, 18'], [Hardwick, Markkanen, Nurmi, 19']

$$V(\Phi) = \frac{1}{64\pi^2} \sum_{\text{bosons}} \left\{ M_{\phi_i}^4 \left[\ln \left(\frac{|M_{\phi_i}^2|}{\mu^2} \right) - \frac{3}{2} \right] + \frac{R_{\mu\nu\rho\sigma} R^{\mu\nu\rho\sigma} - R_{\mu\nu} R^{\mu\nu}}{90} \ln \left(\frac{|M_{\phi_i}^2|}{\mu^2} \right) \right\} \\ - \frac{4}{64\pi^2} \sum_{\text{fermions}} \left\{ M_{\psi_j}^4 \left[\ln \left(\frac{|M_{\psi_j}^2|}{\mu^2} \right) - \frac{3}{2} \right] - \frac{\frac{7}{8} R_{\mu\nu\rho\sigma} R^{\mu\nu\rho\sigma} + R_{\mu\nu} R^{\mu\nu}}{90} \ln \left(\frac{|M_{\psi_j}^2|}{\mu^2} \right) \right\}$$

$$M_{\phi_i}^2 = m^2 + \lambda |\Phi|^2 + \left(\xi - \frac{1}{6}\right) R, \quad M_{\psi_j}^2 = y^2 |\Phi|^2 + \frac{1}{12} R$$

	Inflation	Matter Domination	Radiation Domination
<i>R</i>	$12H_I^2$	$3H^2$	0

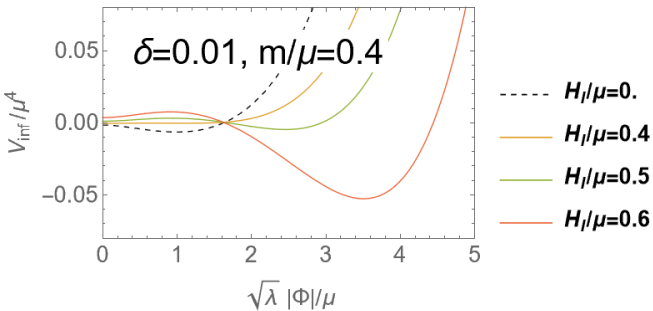


Quasi-SUSY limit:

Potential during inflation (solid lines) is more complicated (as compared to $R = 0$ case, dashed line) and usually has second deeper minimum for bigger value of S

$$S_i^2 \sim \frac{(3 - 12\xi)H_I^2 - m^2}{\delta\lambda}$$

θ_i - "accidental"



Quasi-SUSY limit:

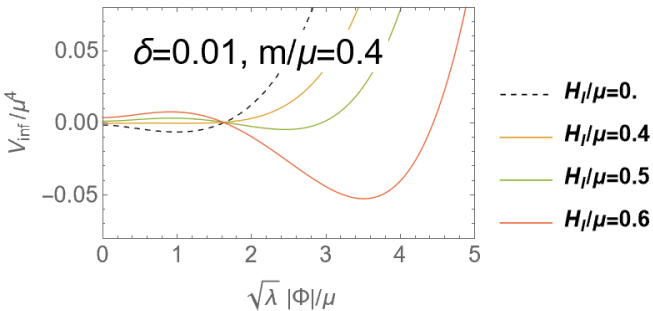
Potential during inflation (solid lines) is more complicated (as compared to $R = 0$ case, dashed line) and usually has second deeper minimum for bigger value of S

$$S_i^2 \sim \frac{(3 - 12\xi)H_I^2 - m^2}{\delta\lambda}$$

θ_i – "accidental"

- **Just after inflation fields S and θ are almost homogeneous**
- **For some time PQ field is almost constant due to Hubble friction**
- **When $H \approx m_S^{\text{eff}}/3$, saxion field S starts to oscillate, and the energy stored transfers to particles mainly via parametric resonance**

→ **produced axions contribute to WDM** [the picture in $\lambda_\phi(S^2 - f_a^2)^2$: Shtanov et al, Kofman et al '94]



Quasi-SUSY limit:

Potential during inflation (solid lines) is more complicated (as compared to $R = 0$ case, dashed line) and usually has second deeper minimum for bigger value of S

$$S_i^2 \sim \frac{(3 - 12\xi)H_i^2 - m^2}{\delta\lambda}$$

θ_i – "accidental"

- Just after inflation fields S and θ are almost homogeneous
- For some time PQ field is almost constant due to Hubble friction
- When $H \approx m_S^{\text{eff}}/3$, saxion field S starts to oscillate, and the energy stored transfers to particles mainly via parametric resonance

→ produced axions contribute to WDM [the picture in $\lambda_\phi(S^2 - f_a^2)^2$: Shtanov et al, Kofman et al '94]

Different corrections to the simple potential may play – sometimes very important – role.

- 1 Introduction
- 2 Radiative corrections
- 3 ϕ evolution during inflation – geometric corrections
- 4 ϕ evolution after inflation – thermal corrections**
- 5 Numerical Results: influence of each correction on axion relics
- 6 Summary and Conclusions

III. Thermal corrections:

Our model

- Thermal effects depend on the same fields ϕ_i, ψ_j and couplings λ, y, m as the CW potential does
- We concentrate on two kinds of thermal effects
 - thermal corrections to the potential of the PQ field
 - thermalization of oscillations

III. Thermal corrections:

Our model

- Thermal effects depend on the same fields ϕ_i, ψ_j and couplings λ, y, m as the CW potential does
- We concentrate on two kinds of thermal effects
 - thermal corrections to the potential of the PQ field
 - thermalization of oscillations
- Typically oscillations of the saxion field, which start at $H \approx \frac{1}{3} m_S^{eff}$, are due to the thermal mass correction
 - Saxion oscillates in potential dominated by thermal mass $\frac{1}{2} \frac{\alpha}{24} T^2 S^2$ term
 - \Rightarrow particle production via parametric resonance very much delayed (because $\dot{\omega}_k / \omega_k^2 \lesssim 1$)

III. Thermal corrections:

Our model

- Thermal effects depend on the same fields ϕ_i, ψ_j and couplings λ, y, m as the CW potential does
- We concentrate on two kinds of thermal effects
 - thermal corrections to the potential of the PQ field
 - thermalization of oscillations
- Typically oscillations of the saxion field, which start at $H \approx \frac{1}{3} m_S^{eff}$, are due to the thermal mass correction
 - Saxion oscillates in potential dominated by thermal mass $\frac{1}{2} \frac{\alpha}{24} T^2 S^2$ term
 - \Rightarrow particle production via parametric resonance very much delayed (because $\dot{\omega}_k / \omega_k^2 \lesssim 1$)
- Resonant production delayed at least until temperature drops below \tilde{T} at which thermal mass domination fades away
- How much has the amplitude of saxion oscillations A_S decreased till such time?

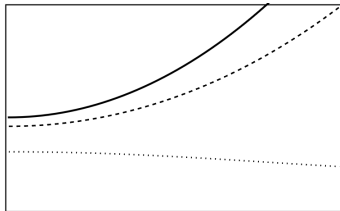
- **Production of cold and warm axions depends strongly on $A_S(\tilde{T})/S_{min,0}$**
 rough estimate $\frac{A_S(\tilde{T})}{S_{min,0}} \approx \mathcal{O}\left(\frac{1}{\sqrt{\epsilon\lambda}} \frac{m}{\mu} \frac{H_I}{10^{18} \text{ GeV}}\right)$
- **scenario "A": $A_S(\tilde{T}) \gg S_{min,0}$**
 - Less warm axions produced (parametric resonance)
- **scenario "B": $A_S(\tilde{T}) \sim S_{min,0}$**
 - More warm axions produced (tachyonic instability)
- **in both scenarios A and B:**
 - Cold axions from misalignment
 - **Saxion oscillations "remember" the initial value θ_i**
 → relic density of cold axions depends on stochastic processes during and before inflation → scale invariant isocurvature CDM perturbations

- **Production of cold and warm axions depends strongly on $A_S(\tilde{T})/S_{min,0}$**

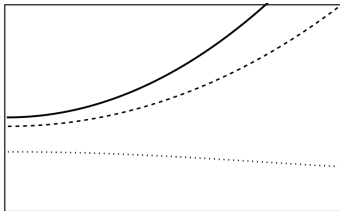
rough estimate $\frac{A_S(\tilde{T})}{S_{min,0}} \approx \mathcal{O}\left(\frac{1}{\sqrt{\epsilon\lambda}} \frac{m}{\mu} \frac{H_I}{10^{18} \text{ GeV}}\right)$

- **scenario "A": $A_S(\tilde{T}) \gg S_{min,0}$**
 - Less warm axions produced (parametric resonance)
- **scenario "B": $A_S(\tilde{T}) \sim S_{min,0}$**
 - More warm axions produced (tachyonic instability)
- **in both scenarios A and B:**
 - Cold axions from misalignment
 - **Saxion oscillations "remember" the initial value θ_i**
 - relic density of cold axions depends on stochastic processes during and before inflation → scale invariant isocurvature CDM perturbations
- **scenario "C": $A_S(\tilde{T}) \ll S_{min,0}$:**
 - Tachyonic instability important
 - **Dynamics may "forget" the initial value θ_i** → if so, relic density of cold axions depends on stochastic processes after inflation → white-noise isocurvature
 - Tachyonic instability makes S oscillations **decay very quickly** [Felder, Garcia-Bellido, Greene, Kofman, Linde, Tkachev, 00'], [Felder, Kofman, Linde, 01']
 - warm axions may be produced depending on details of the $V_{CW}(\Phi)$ potential**

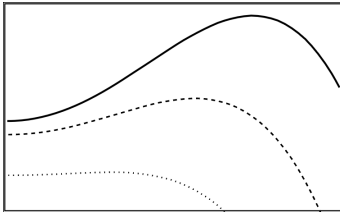
- **C1: no barrier between $S = 0$ and global minimum**
potential which changes with temperature is very shallow at $T \sim \tilde{T}$
 - very few warm axions produced via tachyonic instability



- **C1: no barrier between $S = 0$ and global minimum**
potential which changes with temperature is very shallow at $T \sim \tilde{T}$
 - very few warm axions produced via tachyonic instability



- **C2: barrier between $S = 0$ and global minimum (for a range of temperatures)**
global minimum has a non-negligible depth at tachyonic instability
 - a lot of warm axions produced via tachyonic instability



- 1 Introduction
- 2 Radiative corrections
- 3 ϕ evolution during inflation – geometric corrections
- 4 ϕ evolution after inflation – thermal corrections
- 5 Numerical Results: influence of each correction on axion relics**
- 6 Summary and Conclusions

	λ	δ	m/μ	μ [GeV]	H_I [GeV]	n_{CW}	n_{CW+G}	n_{CW+T}	n_{CW+T+G}
P ₁	10^{-7}	0.1	0.1	10^9	10^{11}	0.042	0.20	$4.57 \cdot 10^5$	$4.57 \cdot 10^5$
P ₂	10^{-7}	0.1	0.1	10^{10}	10^{13}	34	195	$4.33 \cdot 10^5$	$3.18 \cdot 10^5$
P ₃	10^{-7}	0.1	0.1	10^{12}	10^{13}	56	223	$4.28 \cdot 10^5$	$3.04 \cdot 10^5$
P ₄	10^{-7}	0.1	0.1	10^{11}	10^{13}	41.6	206	$4.3 \cdot 10^5$	$3.1 \cdot 10^5$
P ₅	10^{-7}	0.1	0.5	10^{11}	10^{13}	41.9	207	$5.0 \cdot 10^3$	$2.2 \cdot 10^3$
P ₆	10^{-7}	0.1	0.7	10^{11}	10^{13}	42.0	207	95	5.9
P ₇	10^{-7}	0.1	0.8	10^{11}	10^{13}	42.0	207	0	0
P ₈	10^{-7}	0.03	0.5	10^{11}	10^{13}	84	$6.9 \cdot 10^2$	$1.9 \cdot 10^3$	$3.0 \cdot 10^3$
P ₉	10^{-7}	0.01	0.5	10^{11}	10^{13}	$1.6 \cdot 10^2$	$2.0 \cdot 10^3$	$1.2 \cdot 10^3$	$8.9 \cdot 10^3$
P ₁₀	10^{-6}	0.01	0.5	10^{11}	10^{13}	9.0	120	490	47
P ₁₁	10^{-6}	0.001	0.5	10^{11}	10^{13}	36	$1.1 \cdot 10^3$	370	940
P ₁₂	10^{-7}	0.1	0.2	10^{10}	10^{12}	1.3	6.5	$8.4 \cdot 10^4$	$8.3 \cdot 10^4$
P ₁₃	10^{-8}	0.1	0.2	10^{10}	10^{12}	23	120	$2.6 \cdot 10^5$	$2.5 \cdot 10^5$
P ₁₄	10^{-9}	0.1	0.2	10^{10}	10^{12}	$4.2 \cdot 10^2$	$2.1 \cdot 10^3$	$7.9 \cdot 10^5$	$5.8 \cdot 10^5$

Number densities n of warm axions are evaluated at a common T and in units T^3

$$n \rightarrow n(T)/T^3$$

	λ	δ	m/μ	μ [GeV]	H_I [GeV]	n_{CW}	n_{CW+G}	n_{CW+T}	n_{CW+T+G}
P ₁	10^{-7}	0.1	0.1	10^9	10^{11}	0.042	0.20	$4.57 \cdot 10^5$	$4.57 \cdot 10^5$
P ₂	10^{-7}	0.1	0.1	10^{10}	10^{13}	34	195	$4.33 \cdot 10^5$	$3.18 \cdot 10^5$
P ₃	10^{-7}	0.1	0.1	10^{12}	10^{13}	56	223	$4.28 \cdot 10^5$	$3.04 \cdot 10^5$
P ₄	10^{-7}	0.1	0.1	10^{11}	10^{13}	41.6	206	$4.3 \cdot 10^5$	$3.1 \cdot 10^5$
P ₅	10^{-7}	0.1	0.5	10^{11}	10^{13}	41.9	207	$5.0 \cdot 10^3$	$2.2 \cdot 10^3$
P ₆	10^{-7}	0.1	0.7	10^{11}	10^{13}	42.0	207	95	5.9
P ₇	10^{-7}	0.1	0.8	10^{11}	10^{13}	42.0	207	0	0
P ₈	10^{-7}	0.03	0.5	10^{11}	10^{13}	84	$6.9 \cdot 10^2$	$1.9 \cdot 10^3$	$3.0 \cdot 10^3$
P ₉	10^{-7}	0.01	0.5	10^{11}	10^{13}	$1.6 \cdot 10^2$	$2.0 \cdot 10^3$	$1.2 \cdot 10^3$	$8.9 \cdot 10^3$
P ₁₀	10^{-6}	0.01	0.5	10^{11}	10^{13}	9.0	120	490	47
P ₁₁	10^{-6}	0.001	0.5	10^{11}	10^{13}	36	$1.1 \cdot 10^3$	370	940
P ₁₂	10^{-7}	0.1	0.2	10^{10}	10^{12}	1.3	6.5	$8.4 \cdot 10^4$	$8.3 \cdot 10^4$
P ₁₃	10^{-8}	0.1	0.2	10^{10}	10^{12}	23	120	$2.6 \cdot 10^5$	$2.5 \cdot 10^5$
P ₁₄	10^{-9}	0.1	0.2	10^{10}	10^{12}	$4.2 \cdot 10^2$	$2.1 \cdot 10^3$	$7.9 \cdot 10^5$	$5.8 \cdot 10^5$

I. Radiative corrections: may change the amount of warm axions by factor of a few compared to n_{tree} (depending on m/μ , δ and H_I/μ)

	λ	δ	m/μ	μ [GeV]	H_I [GeV]	n_{CW}	n_{CW+G}	n_{CW+T}	n_{CW+T+G}
P ₁	10^{-7}	0.1	0.1	10^9	10^{11}	0.042	0.20	$4.57 \cdot 10^5$	$4.57 \cdot 10^5$
P ₂	10^{-7}	0.1	0.1	10^{10}	10^{13}	34	195	$4.33 \cdot 10^5$	$3.18 \cdot 10^5$
P ₃	10^{-7}	0.1	0.1	10^{12}	10^{13}	56	223	$4.28 \cdot 10^5$	$3.04 \cdot 10^5$
P ₄	10^{-7}	0.1	0.1	10^{11}	10^{13}	41.6	206	$4.3 \cdot 10^5$	$3.1 \cdot 10^5$
P ₅	10^{-7}	0.1	0.5	10^{11}	10^{13}	41.9	207	$5.0 \cdot 10^3$	$2.2 \cdot 10^3$
P ₆	10^{-7}	0.1	0.7	10^{11}	10^{13}	42.0	207	95	5.9
P ₇	10^{-7}	0.1	0.8	10^{11}	10^{13}	42.0	207	0	0
P ₈	10^{-7}	0.03	0.5	10^{11}	10^{13}	84	$6.9 \cdot 10^2$	$1.9 \cdot 10^3$	$3.0 \cdot 10^3$
P ₉	10^{-7}	0.01	0.5	10^{11}	10^{13}	$1.6 \cdot 10^2$	$2.0 \cdot 10^3$	$1.2 \cdot 10^3$	$8.9 \cdot 10^3$
P ₁₀	10^{-6}	0.01	0.5	10^{11}	10^{13}	9.0	120	490	47
P ₁₁	10^{-6}	0.001	0.5	10^{11}	10^{13}	36	$1.1 \cdot 10^3$	370	940
P ₁₂	10^{-7}	0.1	0.2	10^{10}	10^{12}	1.3	6.5	$8.4 \cdot 10^4$	$8.3 \cdot 10^4$
P ₁₃	10^{-8}	0.1	0.2	10^{10}	10^{12}	23	120	$2.6 \cdot 10^5$	$2.5 \cdot 10^5$
P ₁₄	10^{-9}	0.1	0.2	10^{10}	10^{12}	$4.2 \cdot 10^2$	$2.1 \cdot 10^3$	$7.9 \cdot 10^5$	$5.8 \cdot 10^5$

II. Geometric corrections: $n_{CW+G} \gtrsim n_{CW}$ (effect increases with decreasing δ)

- $n_{CW+G}/n_{CW} \sim O(5)$ for $\delta = 0.1$
- $n_{CW+G}/n_{CW} \sim O(30)$ for $\delta = 0.001$

	λ	δ	m/μ	μ [GeV]	H_I [GeV]	n_{CW}	n_{CW+G}	n_{CW+T}	n_{CW+T+G}
P ₁	10^{-7}	0.1	0.1	10^9	10^{11}	0.042	0.20	$4.57 \cdot 10^5$	$4.57 \cdot 10^5$
P ₂	10^{-7}	0.1	0.1	10^{10}	10^{13}	34	195	$4.33 \cdot 10^5$	$3.18 \cdot 10^5$
P ₃	10^{-7}	0.1	0.1	10^{12}	10^{13}	56	223	$4.28 \cdot 10^5$	$3.04 \cdot 10^5$
P ₄	10^{-7}	0.1	0.1	10^{11}	10^{13}	41.6	206	$4.3 \cdot 10^5$	$3.1 \cdot 10^5$
P ₅	10^{-7}	0.1	0.5	10^{11}	10^{13}	41.9	207	$5.0 \cdot 10^3$	$2.2 \cdot 10^3$
P ₆	10^{-7}	0.1	0.7	10^{11}	10^{13}	42.0	207	95	5.9
P ₇	10^{-7}	0.1	0.8	10^{11}	10^{13}	42.0	207	0	0
P ₈	10^{-7}	0.03	0.5	10^{11}	10^{13}	84	$6.9 \cdot 10^2$	$1.9 \cdot 10^3$	$3.0 \cdot 10^3$
P ₉	10^{-7}	0.01	0.5	10^{11}	10^{13}	$1.6 \cdot 10^2$	$2.0 \cdot 10^3$	$1.2 \cdot 10^3$	$8.9 \cdot 10^3$
P ₁₀	10^{-6}	0.01	0.5	10^{11}	10^{13}	9.0	120	490	47
P ₁₁	10^{-6}	0.001	0.5	10^{11}	10^{13}	36	$1.1 \cdot 10^3$	370	940
P ₁₂	10^{-7}	0.1	0.2	10^{10}	10^{12}	1.3	6.5	$8.4 \cdot 10^4$	$8.3 \cdot 10^4$
P ₁₃	10^{-8}	0.1	0.2	10^{10}	10^{12}	23	120	$2.6 \cdot 10^5$	$2.5 \cdot 10^5$
P ₁₄	10^{-9}	0.1	0.2	10^{10}	10^{12}	$4.2 \cdot 10^2$	$2.1 \cdot 10^3$	$7.9 \cdot 10^5$	$5.8 \cdot 10^5$

III. Thermal corrections: **Scenario C2(barrier)**

$$n_{CW+T}, n_{CW+T+G} \gg n_{CW}$$

	λ	δ	m/μ	μ [GeV]	H_I [GeV]	n_{CW}	n_{CW+G}	n_{CW+T}	n_{CW+T+G}
P ₁	10^{-7}	0.1	0.1	10^9	10^{11}	0.042	0.20	$4.57 \cdot 10^5$	$4.57 \cdot 10^5$
P ₂	10^{-7}	0.1	0.1	10^{10}	10^{13}	34	195	$4.33 \cdot 10^5$	$3.18 \cdot 10^5$
P ₃	10^{-7}	0.1	0.1	10^{12}	10^{13}	56	223	$4.28 \cdot 10^5$	$3.04 \cdot 10^5$
P ₄	10^{-7}	0.1	0.1	10^{11}	10^{13}	41.6	206	$4.3 \cdot 10^5$	$3.1 \cdot 10^5$
P ₅	10^{-7}	0.1	0.5	10^{11}	10^{13}	41.9	207	$5.0 \cdot 10^3$	$2.2 \cdot 10^3$
P ₆	10^{-7}	0.1	0.7	10^{11}	10^{13}	42.0	207	95	5.9
P ₇	10^{-7}	0.1	0.8	10^{11}	10^{13}	42.0	207	0	0
P ₈	10^{-7}	0.03	0.5	10^{11}	10^{13}	84	$6.9 \cdot 10^2$	$1.9 \cdot 10^3$	$3.0 \cdot 10^3$
P ₉	10^{-7}	0.01	0.5	10^{11}	10^{13}	$1.6 \cdot 10^2$	$2.0 \cdot 10^3$	$1.2 \cdot 10^3$	$8.9 \cdot 10^3$
P ₁₀	10^{-6}	0.01	0.5	10^{11}	10^{13}	9.0	120	490	47
P ₁₁	10^{-6}	0.001	0.5	10^{11}	10^{13}	36	$1.1 \cdot 10^3$	370	940
P ₁₂	10^{-7}	0.1	0.2	10^{10}	10^{12}	1.3	6.5	$8.4 \cdot 10^4$	$8.3 \cdot 10^4$
P ₁₃	10^{-8}	0.1	0.2	10^{10}	10^{12}	23	120	$2.6 \cdot 10^5$	$2.5 \cdot 10^5$
P ₁₄	10^{-9}	0.1	0.2	10^{10}	10^{12}	$4.2 \cdot 10^2$	$2.1 \cdot 10^3$	$7.9 \cdot 10^5$	$5.8 \cdot 10^5$

III. Thermal corrections: **Scenario C2(barrier)**

$$n_{CW+T}, n_{CW+T+G} \gg n_{CW}$$

- Strong dependence on m/μ
- scenarios C2 \rightarrow C1 (e.g. P₆)

	λ	δ	m/μ	μ [GeV]	H_I [GeV]	n_{CW}	n_{CW+G}	n_{CW+T}	n_{CW+T+G}
P ₁	10^{-7}	0.1	0.1	10^9	10^{11}	0.042	0.20	$4.57 \cdot 10^5$	$4.57 \cdot 10^5$
P ₂	10^{-7}	0.1	0.1	10^{10}	10^{13}	34	195	$4.33 \cdot 10^5$	$3.18 \cdot 10^5$
P ₃	10^{-7}	0.1	0.1	10^{12}	10^{13}	56	223	$4.28 \cdot 10^5$	$3.04 \cdot 10^5$
P ₄	10^{-7}	0.1	0.1	10^{11}	10^{13}	41.6	206	$4.3 \cdot 10^5$	$3.1 \cdot 10^5$
P ₅	10^{-7}	0.1	0.5	10^{11}	10^{13}	41.9	207	$5.0 \cdot 10^3$	$2.2 \cdot 10^3$
P ₆	10^{-7}	0.1	0.7	10^{11}	10^{13}	42.0	207	95	5.9
P ₇	10^{-7}	0.1	0.8	10^{11}	10^{13}	42.0	207	0	0
P ₈	10^{-7}	0.03	0.5	10^{11}	10^{13}	84	$6.9 \cdot 10^2$	$1.9 \cdot 10^3$	$3.0 \cdot 10^3$
P ₉	10^{-7}	0.01	0.5	10^{11}	10^{13}	$1.6 \cdot 10^2$	$2.0 \cdot 10^3$	$1.2 \cdot 10^3$	$8.9 \cdot 10^3$
P ₁₀	10^{-6}	0.01	0.5	10^{11}	10^{13}	9.0	120	490	47
P ₁₁	10^{-6}	0.001	0.5	10^{11}	10^{13}	36	$1.1 \cdot 10^3$	370	940
P ₁₂	10^{-7}	0.1	0.2	10^{10}	10^{12}	1.3	6.5	$8.4 \cdot 10^4$	$8.3 \cdot 10^4$
P ₁₃	10^{-8}	0.1	0.2	10^{10}	10^{12}	23	120	$2.6 \cdot 10^5$	$2.5 \cdot 10^5$
P ₁₄	10^{-9}	0.1	0.2	10^{10}	10^{12}	$4.2 \cdot 10^2$	$2.1 \cdot 10^3$	$7.9 \cdot 10^5$	$5.8 \cdot 10^5$

III. Thermal corrections: **Scenario C1 (no barrier)**

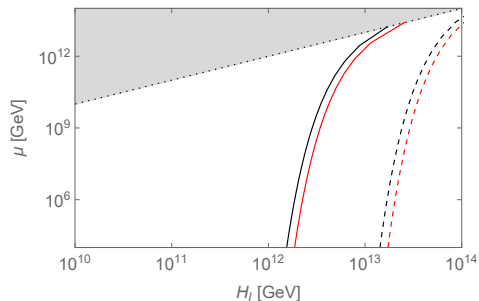
$$n_{CW+T}, n_{CW+T+G} \approx 0$$

- 1 Introduction
- 2 Radiative corrections
- 3 ϕ evolution during inflation – geometric corrections
- 4 ϕ evolution after inflation – thermal corrections
- 5 Numerical Results: influence of each correction on axion relics
- 6 Summary and Conclusions**

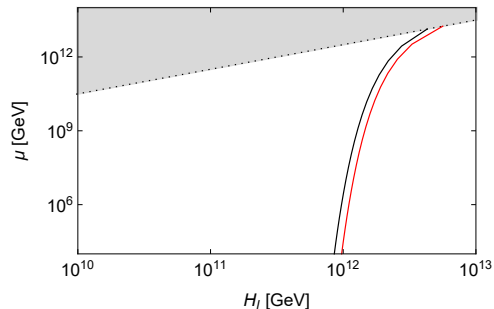
- Non-trivial dynamics of Peccei-Quinn requires extremely small self-coupling
- Crucial role is played by various corrections:
 - radiative, geometric, and thermal
- During inflation
 - saxion potential has (second) minimum at $S \gg S_{min,0}$
 - $\langle S_i \rangle$, $\langle \theta_i \rangle$, $\langle \delta S_i^2 \rangle$, $\langle \delta \theta_i^2 \rangle$ determined by quantum fluctuations during inflation
 - $\langle S_i \rangle$ close to the position of the minimum at $S \gg S_{min,0}$
 - constraints from DM isocurvature relaxed
 - very long inflation not needed?
- After inflation
 - thermal corrections are very important for the evolution of saxion field S
 - production of axions can be via parametric resonance or tachyonic instability, and it depends quite strongly on details of a model
 - axion contribution to WDM may vary by many orders of magnitude
 - isocurvature perturbations of axion CDM may be standard (scale-invariant generated during inflation) or may have the form of white noise
- Numerical simulations necessary for precise predictions

BACK UP

MD($\lambda = 10^{-7}$, $\delta = 0.1$)



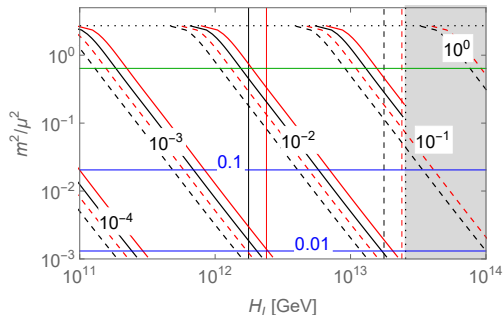
RD($\lambda = 10^{-10}$, $\delta = 10^{-2}$)



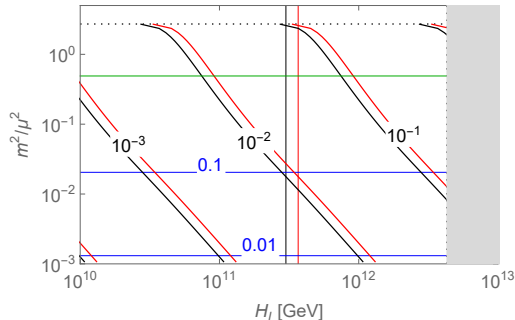
For parameters to the left from the black/red solid lines, the S oscillations start due to the thermal mass

Some examples – lines of constant $A_S(\tilde{T})/S_{\min,0}$

MD ($\lambda = 10^{-7}$, $\delta = 0.1$)



RD ($\lambda = 10^{-10}$, $\delta = 10^{-2}$)



- ⇒ scenario B typically only when both H_I and m/μ are \sim maximal allowed
- ⇒ scenario C typically when either H_I or m/μ is smaller

	λ	δ	m/μ	μ [GeV]	H_I [GeV]	n_{CW}	n_{CW+G}	n_{CW+T}	n_{CW+T+G}
P ₁	10^{-7}	0.1	0.1	10^9	10^{11}	0.042	0.20	$4.57 \cdot 10^5$	$4.57 \cdot 10^5$
P ₂	10^{-7}	0.1	0.1	10^{10}	10^{13}	34	195	$4.33 \cdot 10^5$	$3.18 \cdot 10^5$
P ₃	10^{-7}	0.1	0.1	10^{12}	10^{13}	56	223	$4.28 \cdot 10^5$	$3.04 \cdot 10^5$
P ₄	10^{-7}	0.1	0.1	10^{11}	10^{13}	41.6	206	$4.3 \cdot 10^5$	$3.1 \cdot 10^5$
P ₅	10^{-7}	0.1	0.5	10^{11}	10^{13}	41.9	207	$5.0 \cdot 10^3$	$2.2 \cdot 10^3$
P ₆	10^{-7}	0.1	0.7	10^{11}	10^{13}	42.0	207	95	5.9
P ₇	10^{-7}	0.1	0.8	10^{11}	10^{13}	42.0	207	0	0
P ₈	10^{-7}	0.03	0.5	10^{11}	10^{13}	84	$6.9 \cdot 10^2$	$1.9 \cdot 10^3$	$3.0 \cdot 10^3$
P ₉	10^{-7}	0.01	0.5	10^{11}	10^{13}	$1.6 \cdot 10^2$	$2.0 \cdot 10^3$	$1.2 \cdot 10^3$	$8.9 \cdot 10^3$
P ₁₀	10^{-6}	0.01	0.5	10^{11}	10^{13}	9.0	120	490	47
P ₁₁	10^{-6}	0.001	0.5	10^{11}	10^{13}	36	$1.1 \cdot 10^3$	370	940
P ₁₂	10^{-7}	0.1	0.2	10^{10}	10^{12}	1.3	6.5	$8.4 \cdot 10^4$	$8.3 \cdot 10^4$
P ₁₃	10^{-8}	0.1	0.2	10^{10}	10^{12}	23	120	$2.6 \cdot 10^5$	$2.5 \cdot 10^5$
P ₁₄	10^{-9}	0.1	0.2	10^{10}	10^{12}	$4.2 \cdot 10^2$	$2.1 \cdot 10^3$	$7.9 \cdot 10^5$	$5.8 \cdot 10^5$

P₈, P₉, P₁₁– scenario B, $n_{CW+T}, n_{CW+T+G} \gg n_{CW}$

	λ	δ	m/μ	μ [GeV]	H_I [GeV]	n_{CW}	n_{CW+G}	n_{CW+T}	n_{CW+T+G}
P ₁	10^{-7}	0.1	0.1	10^9	10^{11}	0.042	0.20	$4.57 \cdot 10^5$	$4.57 \cdot 10^5$
P ₂	10^{-7}	0.1	0.1	10^{10}	10^{13}	34	195	$4.33 \cdot 10^5$	$3.18 \cdot 10^5$
P ₃	10^{-7}	0.1	0.1	10^{12}	10^{13}	56	223	$4.28 \cdot 10^5$	$3.04 \cdot 10^5$
P ₄	10^{-7}	0.1	0.1	10^{11}	10^{13}	41.6	206	$4.3 \cdot 10^5$	$3.1 \cdot 10^5$
P ₅	10^{-7}	0.1	0.5	10^{11}	10^{13}	41.9	207	$5.0 \cdot 10^3$	$2.2 \cdot 10^3$
P ₆	10^{-7}	0.1	0.7	10^{11}	10^{13}	42.0	207	95	5.9
P ₇	10^{-7}	0.1	0.8	10^{11}	10^{13}	42.0	207	0	0
P ₈	10^{-7}	0.03	0.5	10^{11}	10^{13}	84	$6.9 \cdot 10^2$	$1.9 \cdot 10^3$	$3.0 \cdot 10^3$
P ₉	10^{-7}	0.01	0.5	10^{11}	10^{13}	$1.6 \cdot 10^2$	$2.0 \cdot 10^3$	$1.2 \cdot 10^3$	$8.9 \cdot 10^3$
P ₁₀	10^{-6}	0.01	0.5	10^{11}	10^{13}	9.0	120	490	47
P ₁₁	10^{-6}	0.001	0.5	10^{11}	10^{13}	36	$1.1 \cdot 10^3$	370	940
P ₁₂	10^{-7}	0.1	0.2	10^{10}	10^{12}	1.3	6.5	$8.4 \cdot 10^4$	$8.3 \cdot 10^4$
P ₁₃	10^{-8}	0.1	0.2	10^{10}	10^{12}	23	120	$2.6 \cdot 10^5$	$2.5 \cdot 10^5$
P ₁₄	10^{-9}	0.1	0.2	10^{10}	10^{12}	$4.2 \cdot 10^2$	$2.1 \cdot 10^3$	$7.9 \cdot 10^5$	$5.8 \cdot 10^5$

P₈, P₉, P₁₁– scenario B, geometric correction increase n : $n_{CW+T} \lesssim n_{CW+T+G}$

	λ	δ	m/μ	μ [GeV]	H_I [GeV]	n_{CW}	n_{CW+G}	n_{CW+T}	n_{CW+T+G}
P ₁	10^{-7}	0.1	0.1	10^9	10^{11}	0.042	0.20	$4.57 \cdot 10^5$	$4.57 \cdot 10^5$
P ₂	10^{-7}	0.1	0.1	10^{10}	10^{13}	34	195	$4.33 \cdot 10^5$	$3.18 \cdot 10^5$
P ₃	10^{-7}	0.1	0.1	10^{12}	10^{13}	56	223	$4.28 \cdot 10^5$	$3.04 \cdot 10^5$
P ₄	10^{-7}	0.1	0.1	10^{11}	10^{13}	41.6	206	$4.3 \cdot 10^5$	$3.1 \cdot 10^5$
P ₅	10^{-7}	0.1	0.5	10^{11}	10^{13}	41.9	207	$5.0 \cdot 10^3$	$2.2 \cdot 10^3$
P ₆	10^{-7}	0.1	0.7	10^{11}	10^{13}	42.0	207	95	5.9
P ₇	10^{-7}	0.1	0.8	10^{11}	10^{13}	42.0	207	0	0
P ₈	10^{-7}	0.03	0.5	10^{11}	10^{13}	84	$6.9 \cdot 10^2$	$1.9 \cdot 10^3$	$3.0 \cdot 10^3$
P ₉	10^{-7}	0.01	0.5	10^{11}	10^{13}	$1.6 \cdot 10^2$	$2.0 \cdot 10^3$	$1.2 \cdot 10^3$	$8.9 \cdot 10^3$
P ₁₀	10^{-6}	0.01	0.5	10^{11}	10^{13}	9.0	120	490	47
P ₁₁	10^{-6}	0.001	0.5	10^{11}	10^{13}	36	$1.1 \cdot 10^3$	370	940
P ₁₂	10^{-7}	0.1	0.2	10^{10}	10^{12}	1.3	6.5	$8.4 \cdot 10^4$	$8.3 \cdot 10^4$
P ₁₃	10^{-8}	0.1	0.2	10^{10}	10^{12}	23	120	$2.6 \cdot 10^5$	$2.5 \cdot 10^5$
P ₁₄	10^{-9}	0.1	0.2	10^{10}	10^{12}	$4.2 \cdot 10^2$	$2.1 \cdot 10^3$	$7.9 \cdot 10^5$	$5.8 \cdot 10^5$

P_{1÷6,10,12÷14} - scenario C2, geometric correction decreases $n : n_{CW+T}$

n_{CW+T+G}

\gtrsim

- thermal corrections neglected – (s)axions produced by parametric resonance:

- $n_{CW+G} \gtrsim n_{CW}$

$$n_{CW} \propto \delta^{-5/8} \lambda^{-5/4} H_I^{3/2} T^3, \quad n_{CW+G} \propto \delta^{-1} \lambda^{-5/4} H_I^{3/2} T^3$$

dependence on m, μ very weak

- thermal corrections accounted – (s)axions produced by tachyonic instability:

- scenario C more natural than B and especially A
- C \rightarrow C1(no barrier), C2(barrier for some T)
- scenario C1 : $n_{CW+T}, n_{CW+T+G} \approx 0$
- scenario C2 : $n_{CW+T}, n_{CW+T+G} \gg n_{CW}$

$$n_{CW+T}, n_{CW+T+G} \propto \lambda^{-1/2} \left(\frac{m}{\mu} \right)^{-2} T^3$$

dependence on δ, μ and H_I much weaker, $n_{CW+T+G} \lesssim n_{CW+T}$

- dedicated numerical computations for C1 – C2 transition region, scenario B ...

scenario D: early thermalization : $T_{\text{th}} > \tilde{T}$

- interactions with thermal plasma – **modification to EOM:**

$$\ddot{S} + (3H + \Gamma_{\text{th}}) \dot{S} + \frac{\partial V_{\text{eff}}}{\partial S} = 0$$

$$\Gamma_{\text{th}}^{(\phi)} \sim \frac{\lambda^2 S^2}{\alpha_{\text{th}} T}, \quad \Gamma_{\text{th}}^{(\psi)} \sim y^2 \alpha_{\text{th}} T$$

$$\Rightarrow T_{\text{th}} \sim \sqrt{\frac{45}{4\pi^3 g_*}} \alpha_{\text{th}} \lambda M_{Pl}$$

early thermalization if:

$$\frac{m^2}{\mu^2} \ln \left(\frac{e\mu^2}{m^2} \right) \lesssim \frac{15 n_{\text{eff}}(\tilde{T})}{\pi g_* N_s} \alpha_{\text{th}}^2 \lambda^2 \frac{M_{Pl}^2}{\mu^2}$$

$\alpha_{\text{th}} = \alpha_s \sim 0.1 \Rightarrow$ **RHS bigger than 1, if $\mu \lesssim \lambda \cdot 10^{17}$ GeV**

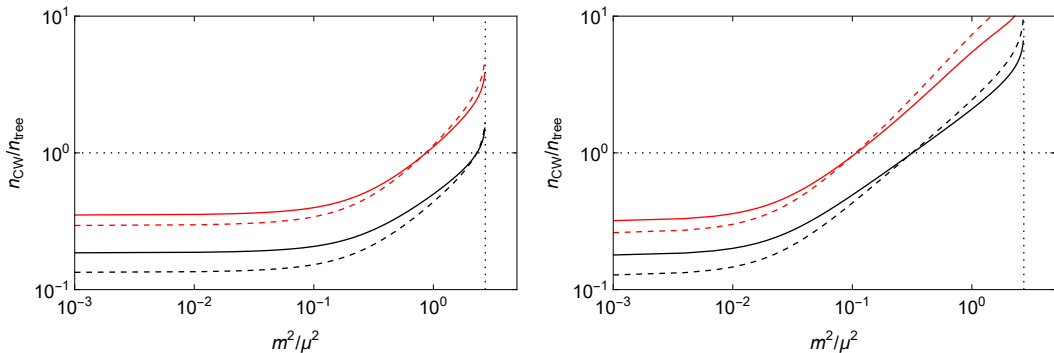


Figure: The ratio of densities of warm axions produced via a parametric resonance with (n_{CW}) and without (n_{tree}) radiative corrections taken into account as a function of m^2/μ^2 . The relevant parameters are fixed as: $\delta = 0.1$ (left panel) and $\delta = 0.01$ (right panel); $H_I/\mu = 5$ (red curves) and $H_I/\mu = 10^3$ (black curves). The solid (dashed) lines correspond to situation when the axions are produced after (before) the end of the reheating process.

- We will focus on

- CW with only geometric corrections ($CW + G$)
- CW with only thermal corrections ($CW + T$)
- CW with both geometric and thermal corrections ($CW + T + G$)

n_{CW} , n_{CW+G} , n_{CW+T} and n_{CW+T+G} are rescaled to a common T (in units T^3)

n_{CW} vs n_{tree} : $n_{CW}/n_{tree} \lesssim 1$ depending on m/μ , δ and H_I/μ

- Two different approximations:

-

$$n_{CW}, n_{CW+G} \sim \frac{1}{2} \frac{V_{CW}}{m_S} \Big|_{S=S_i} \quad (\text{parametric resonance})$$

-

$$n_{CW+T}, n_{CW+T+G} \sim \frac{1}{2} \frac{\Delta V_{tot}}{m_S} \Big|_{T \sim \tilde{T}} \quad (\text{tachyonic instability})$$

ΔV_{tot} = (available potential energy), m_S = (mass at the global minimum)

- Cold axions produced via the conventional misalignment mechanism
- $n_{a, cold}$ often determined by stochastic processes during inflation...
...despite $V_{full}(\Phi)$ is in the unbroken phase for some time

saxion keeps oscillating and carries the initial PQ phase θ_i

- in the end one should compare

$$\rho_{a, warm} + \rho_{a, cold} \leftrightarrow \rho_{DM, observed}$$

⇒ extra flexibility:

if $\rho_{a, warm}$ too small (or vanishing...), often possible to complement with $\rho_{a, cold}$ (choice of θ_i)

Number densities (n.d.) of ALP WDM n_i (in units T^3):

- ① **radiative corrections: n_{CW} vs n_{tree} : $n_{CW}/n_{tree} \lesssim 1$**
(depending on m/μ , δ and H_I/μ)
 - $n_{CW} \equiv$ (n.d. of warm ALP for "pure" CW potential)
 - $n_{tree} \equiv$ (n.d. of warm ALP for the *corresponding* Mexican hat potential)
- ② **We will take n_{CW} as the reference and compare it with:**
 - $n_{CW+G} \equiv$ (CW with only geometric corrections)
 - $n_{CW+T} \equiv$ (CW with only thermal corrections)
 - $n_{CW+T+G} \equiv$ (CW with both geometric and thermal corrections)

n_{CW} , n_{CW+G} , n_{CW+T} and n_{CW+T+G} are rescaled to a common T

- **We use the full thermal potential**

$$V_T(\Phi) = \frac{T^4}{2\pi^2} \left[\sum_{\text{bosons}} J_+ \left(\frac{M_{\phi_i}}{T} \right) + 4 \sum_{\text{fermions}} J_- \left(\frac{M_{\psi_j}}{T} \right) \right]$$

$$J_{\pm}(y) = \pm \int_0^{\infty} x^2 \ln \left[1 \mp \exp \left(-\sqrt{x^2 + y^2} \right) \right] dx$$

Number densities (n.d.) of ALP WDM n_i :

- ① **radiative corrections: n_{CW} vs n_{tree} : $n_{CW}/n_{tree} \lesssim 1$**
(depending on m/μ , δ and H_I/μ)
 - $n_{CW} \equiv$ (n.d. of warm ALP for "pure" Gildener-Weinberg potential)
 - $n_{tree} \equiv$ (n.d. of warm ALP for the *corresponding* Mexican hat potential)
- ② **We will take n_{CW} as the reference and compare it with:**
 - $n_{CW+G} \equiv$ (CW with only geometric corrections)
 - $n_{CW+T} \equiv$ (CW with only thermal corrections)
 - $n_{CW+T+G} \equiv$ (CW with both geometric and thermal corrections)

n_{CW} , n_{CW+G} , n_{CW+T} and n_{CW+T+G} are rescaled to a common T (and in units T^3)